2013 21st Mediterranean Conference on Control & Automation (MED)
Platanias-Chania, Crete, Greece, June 25-28, 2013

Guidance, Navigation, and Control of an Unmanned Hovercraft

Kilsoo Kim, Young-Ki Lee, Sehwan Oh, David Moroniti, *Members, IEEE*, Dimitri Mavris, and George J. Vachtsevanos, *Senior Members, IEEE,* Nikos Papamarkos*, Member, IEEE,*George Georgoulas, *Member, IEEE*

Abstract— **This paper introduces a simulation and evaluation of guidance, navigation, and control algorithms applied to an autonomous hovercraft. A line-of-sight guidance law is adopted in conjunction with a neural network based adaptive dynamic inversion control scheme for the underactuated hovercraft following a prescribed path. The simulation result demonstrates that the guidance and control scheme can be effective in waypoint following of the underactuated hovercraft, especially, when external disturbances exist. It is also shown that the error signals are bounded using Lyapunov's direct method.**

I. INTRODUCTION

Underactuated mechanical systems have fewer control inputs than configuration variables. They appear in a broad range of applications including a large array of robotics, aerospace, transportation and marine systems. The study of those systems is motivated by the fact that it is more cost effective and practical due to its weight, complexity, and efficiency than the fully actuated system. A class of underactuated marine systems poses considerable challenges in control system design due to its complex hydrodynamic effects. Hovercraft belong to the same marine vessel category with similar structure models.

The motion control laws of underactuated systems are divided into the following categories: setpoint control, trajectory tracking control, and path following control. Setpoint control is required for dynamic positioning of vessels in fixed target operations such as autonomous docking. Due to the nature of underactuated systems, the surface vessel setpoint control approaches are only presented as either discontinuous [1-5] or continuous time-varying control laws [6-17]. Trajectory tracking control [14, 18-34] is concerned with the design of control laws that force a vehicle to reach and follow a time parameterized reference whereas path following control [35-46] methods follow a predefined path that involves only a spatial constraint. Common to all such systems is the lack of a comprehensive and practical control law that is robust to uncertainties and disturbances associated with the surface vessel and its environment. There is also a lack of experimental studies for setpoint stabilization [3, 11-13] and trajectory tracking/path following [19, 29, 31, 36, 37, 39, 44].

Traditional trajectory tracking methods combine the positional and temporal requirements into one single assignment when the geometrical path is specified by a path planner and is completely known in advance. These schemes do not utilize the geometrical information that may significantly degrade the transient convergent behavior of the vessel's position. This paper presents a guidance-based path following methodology to address the general guidance and control problem as an alternative to classical trajectory tracking methods.

A. *Previous Path Following Work*

Skjetne and Fossen [43] proposed a three-step backstepping method by decoupling the surge motion from the sway dynamics and deriving an independent control law to keep a nearly constant surge speed. For maneuvering experiments with a small ship in a marine control laboratory, Skjetne et al. [44] modeled, identified, and designed a basic controller based on a more general robust output maneuvering technique, described in [47]. Ihle et al. [40] developed an output feedback controller using an observer backstepping approach that applies damping terms to counteract disturbances to the controller by transforming the problem into an output feedback form where nonlinearities only appear in the output.

Do et al. [36] developed a backstepping control law based on Lyapunov's direct method for a ship with non-vanishing uncertainties. They mentioned that yaw dynamics discontinuities could cause difficulties in applying the backstepping technique. Do and Pan [37] extended their previous work to a more comprehensive control law and its experimental implementation on a small model ship. The control law includes non-diagonal inertia, drag matrices, and nonlinear quadratic drag terms, as well as environmental disturbances. The experimental results showed consistent chattering in the surge and yaw motion in following a sinusoidal path, a straight line, and a circular path. For the same model as [37] Do and Pan also show similar performance by proposing a global robust and adaptive path following control law [38].

Burger et al. [35] proposed a control law for straight line path following of formations of underactuated surface vessels under the influence of ocean currents and presented successful simulation results. Li et al. [41] proposed a path following controller based on a linear model predictive control with a linearized 4-DOF model where actuator and roll constraints are imposed in simulation. However, the surge speed is assumed to be constant and surge dynamics are neglected. Sorensen et al. [45] proposed a linear quadratic feedback

Kilsoo Kim, Young-Ki Lee, Sehwan Oh, David Moroniti, and Dimitri Mavris are with the School of Aerospace Engineering, Georgia Institute of Technology, Atlanta, GA 30332 USA (phone: 404-894-1557; fax: 404-894-6596; e-mail: (kkim, ylee, soh, and dmoroni@asdl.gatech.edu, dimitri.mavris@aerospace.gatech.edu).

George J. Vachtsevanos is with the School of Electrical and Computer Engineering, Georgia Institute of Technology, Atlanta, GA 30332 USA (phone: 404-894-6252; fax: 404-894-7583; e-mail: gjv@ece.gatech.edu).

Nikos Papamarkos is with the Democritus University of Thrace, Greece (e-mail:papamark@ee.duth.gr).

George Georgoulas is with KIC Laboratory, Department of Informatics and Telecommunications Technology, Technological Educational Institute of Epirus, GR-47100, Greece (e-mail: georgoul@teleinfom.teiep.gr).

controller for station keeping and tracking where a reference model calculates the reference trajectory and wave/wind disturbances; experimental ship data are used to demonstrate the controller performance. McNinch et al. [46] considered a nonlinear model predictive control approach with power law drag terms in an autonomous recovery scenario distinguishing between the vessel forward and backward motion dynamics.

Fredriksen and Pettersen [39] proposed a global exponential path following control law for way point maneuvering of underactuated vessels by using a line-of-sight approach to define the desired yaw angle and parameterize the path to derive a stabilizing speed control law for surge motion. Experimental results are relatively successful with a controller based on a linear damping model. Another path following control approach employing a way-point guidance scheme based on line-of-sight projection was proposed by Moreira et al. [42]. To improve the speed of convergence to the desired path, the approach was based on the calculation of a dynamic line-of-sight vector. The speed controller was developed using feedback linearization considering water current and wind disturbances.

B. Neural Network based Adaptive Dynamic Inversion

Using nonlinear transformation techniques, the state and/or control of the nonlinear system can be transformed to linear dynamics such that linear methods can then be applied and subsequently converted back into the original coordinates via an inverse transformation. This broad class of techniques known as feedback linearization found comprehensive treatments by Isidori [48], Meyer and Cicolani [49], and Menon et al. [50]. Dynamic inversion, known as a specific case of feedback linearization, has been investigated in an application to super-maneuverable aircraft [51-53], where it was shown to be an effective way of compensating for the nonlinearities. However, the nonlinear control techniques, such as dynamic inversion, require the accurate knowledge of the plant dynamics and were shown to be vulnerable to modeling errors by Brinker and Wise [54]. For robust nonlinear control techniques one requires robustness to sources of uncertainty including unmodeled dynamics, parametric uncertainty, and uncertain nonlinearities [54-56].

Artificial Neural Networks (ANNs) are known for their ability to approximate uncertain nonlinear mappings to a high degree of accuracy and has come to be seen as a potential solution to many outstanding problems in adaptive robust control of nonlinear systems [57, 58]. Adaptive control has been derived from Lyapunov stability theory. Parameter adaptive control schemes may be divided into direct and indirect. Indirect adaptive control involves on-line identification of plant parameters, on the basis of a suitable control law is implemented. In the case of direct adaptive control, the parameters defining the controller are updated directly. Several efforts concentrate specifically on adaptive control of feedback-linearizable systems [59, 60].

This paper is focused on the use of a direct NN based adaptive control architecture that compensates for unknown plant nonlinearities in a feedback linearizing control framework. For the underactuated hovercraft, the guidance system should generate appropriate command to regulate all degrees of freedom, so that the commands (desirable surge speed and yaw angle) are generated from the line-of-sight (LOS) guidance law. This LOS guidance law is combined with NN based adaptive dynamic inversion mode for the vehicle to follow a set of waypoints and dock near the final waypoint.

The paper is organized as follows: Section II provides notation used through this paper. Section III represents the hovercraft model focusing on its kinematic and dynamics with uncertainty. In Section IV, the guidance, navigation, and control laws for the hovercraft are derived. Section V provides the boundedness of error dynamics. Section VI illustrates the simulation results. Finally, Section VII concludes with a brief discussion of the results and future research work.

II. NOTATION

Throughout this paper $\mathbb{R}$ denotes the set of real numbers, $\mathbb{R}^n$ denotes the set of $n \times 1$ real column vectors, $\mathbb{R}^{n\times m}$ denotes the set of $n \times m$ real matrices, $\lambda_{\min}(A)$ denotes the minimum eigenvalue of the Hermitian matrix A, $\mathrm{tr}(\cdot)$ represents the trace operator. $|\cdot|$ and $\|\cdot\|_F$ denote the Euclidian vector norm and the Frobenius matrix norm, respectively. Furthermore, $(\cdot)^T$ denotes the transpose, $(\cdot)^{-1}$ denotes the inverse, $\equiv$ denotes the equality by definition, $0_{n\times m}$ denotes $n \times m$ zero matrix, $(\dot{\cdot})$ denotes time derivative of $(\cdot)$, and $\forall$x represents for all x . For simplicity, $(\cdot)$ usually indicates a time-varying signal $(\cdot)(t)$.

III. HOVERCRAFT MODEL

The first step towards the development of the hovercraft's equations of motion is the definition of two reference frames. Each frame is characterized by its center and three mutually orthonormal vectors shown in Figure 1. The first one is the inertial frame defined as $\mathcal{F}_I = \{O_I, \vec{\imath}_I, \vec{\jmath}_I, \vec{k}_I\}$. A typical convention of the inertial frame is the North-East-Down system where $\vec{\imath}_I$ points North, $\vec{\jmath}_I$ points East, and $\vec{k}_I$ points at the center of the Earth. The second frame is the body-fixed reference frame defined as $\mathcal{F}_B = \{O_B, \vec{\imath}_B, \vec{\jmath}_B, \vec{k}_B\}$, where the center O_B is located at the Center of Gravity of the hovercraft. The vector $\vec{\imath}_B$ points forward, $\vec{\jmath}_B$ points at the aft right side of the hovercraft and $\vec{k}_B$ points downward such that $\{\vec{\imath}_B, \vec{\jmath}_B, \vec{k}_B\}$ constitutes a right handed Cartesian coordinate frame. The 3-DOF model of the underactuated hovercraft moving on the two-dimensional space shown in Figure 1 considers only surge (u), sway (v), and yaw (ψ) motion. The motions of roll, heave, and pitch are neglected. The vehicle's kinematic equation between the inertial reference frame and the body-fixed frame is expressed as

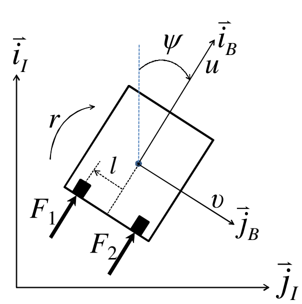

Figure 1. Schematic of the hovercraft in earth-fixed and body-fixed frames.

$$\dot{\eta} = R(\psi)\nu \tag{1}$$

where $\eta = [x, y, \psi]^T \in \mathbb{R}^3$; x and y are the Cartesian coordinates of the center of mass; ψ defines the vehicle's orientation; $\nu = [u, v, r]^T \in \mathbb{R}^3$; r is its angular speed; u and v are surge and sway speed, respectively in the body fixed frame. The rotation matrix is

$$R(\psi) = \begin{bmatrix} \cos\psi & -\sin\psi & 0 \\ \sin\psi & \cos\psi & 0 \\ 0 & 0 & 1 \end{bmatrix} \tag{2}$$

The equation of motion can be written as

$$\dot{\mathrm{v}} + f(\mathrm{v}) + \Delta(\mathrm{x}) = \tau \tag{3}$$

where $\mathrm{x} = [\eta^T, \mathrm{v}^T]^T \in \mathbb{R}^6$ and

$$\begin{aligned} f(\mathrm{v}) &\equiv [f_u(\mathrm{v}), f_v(\mathrm{v}), f_r(\mathrm{v})]^T \\ &= \left[-vr + \frac{d_u}{m}u, ur + \frac{d_v}{m}v, \frac{d_r}{J}r\right]^T \\ \tau \equiv [\tau_u, 0, \tau_r]^T &= \left[\frac{(F_1 + F_2)}{m}, 0, \frac{l(F_1 - F_2)}{J}\right]^T \end{aligned} \tag{4}$$

where m is the vehicle's mass, J is its rotational mass moment of inertia, and d_u, d_v, and d_r are the coefficients of viscous and rotational friction, respectively. F_1 and F_2 are fan forces, l denotes the moment arm of the forces with respect to the center of geometry and mass of the vehicle, which are assumed to coincide. $\Delta(\mathrm{x})$ represents the uncertainties stemming from modeling error/nonlinearity and external disturbances and is assumed to be linearly parameterized

$$\Delta(\mathrm{x}) = W^T\beta(\mathrm{x}) + \varepsilon(\mathrm{x}), \qquad \forall \mathrm{x} \in D_{\mathrm{x}} \tag{5}$$

where $W \in \mathbb{R}^{s\times 3}$ is an unknown constant ideal weight matrix that satisfies $\|W\|_F = w^*$, $\beta(\cdot): \mathbb{R}^6 \to \mathbb{R}^s$ is a known basis vector of the form $\beta(\mathrm{x}) = [\beta_1(\mathrm{x}), \beta_2(\mathrm{x}), \dots, \beta_s(\mathrm{x})]^T$, and ε is the residual error satisfying $|\varepsilon| < \epsilon$ for a sufficiently large domain $D_{\mathrm{x}} \subset \mathbb{R}^6$.

IV. Guidance, Navigation, and Control

For the underactuated hovercraft, the guidance system should generate appropriate commands to regulate the positions (x, y) and an attitude (ψ). So (u_d, ψ_d) instead of (x_d, y_d, ψ_d) should be generated from the guidance system which uses the pre-defined waypoints set (p_k) and the measured data (η) from navigation system. The computed and low-pass-filtered velocity (ν_{lpf}) of hovercraft is generated from the navigation system which distributes η and ν_{lpf}. Control system generates the required force and moment (τ_u, τ_r) into the hovercraft. The overall flow among the plant, guidance, navigation, and control subsystems is shown in Figure 2.

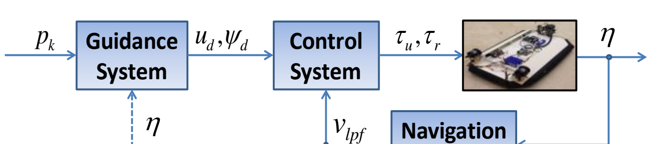

Figure 2. Overall flow in the autonomous hovercraft system.

A. Guidance and Navigation

The following LOS guidance result is adopted from Breivik and Fossen [61]. Consider a straight-line path implicitly defined by two waypoints as shown in Figure 3. Denote these waypoints by $p_k \equiv [x_k, y_k]^T \in \mathbb{R}^2$ and $p_{k+1} \equiv [x_{k+1}, y_{k+1}]^T \in \mathbb{R}^2$, respectively. Also consider a path-fixed reference frame with origin in p_k, whose x-axis has been rotated by a positive angle

$$\alpha_k \equiv \mathrm{atan2}(y_{k+1} - y_k, x_{k+1} - x_k) \tag{6}$$

relative to the x-axis of the stationary reference frame. Therefore, the coordinates of the vehicle kinematic in the path-fixed reference frame can be computed by

$$\varepsilon_l(t) = R(\alpha_k)^T(p(t) - p_k) \tag{7}$$

where $R(\alpha_k) \equiv \begin{bmatrix} \cos\alpha_k & -\sin\alpha_k \\ \sin\alpha_k & \cos\alpha_k \end{bmatrix}$, $\varepsilon_l(t) = [s(t), e_l(t)]^T$ consists of the along-track distance $s(t)$ and the cross-track error $e_l(t)$ shown in Figure 3. The associated control objective for piecewise straight-line path following purposes becomes

$$\lim_{t\to\infty} e_l(t) = 0 \tag{8}$$

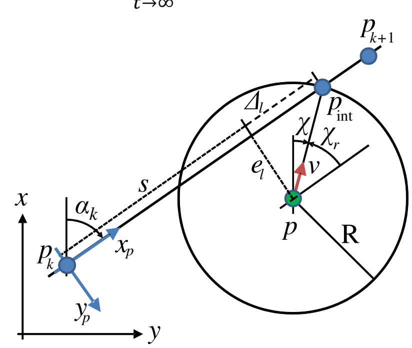

Figure 3. Main variables associated with LOS steering laws.

The steering assignment is separated into two parts

$$\chi(e_l) = \chi_p + \chi_r(e_l) \tag{9}$$

where $\chi_p = \alpha_k$ is the path-tangential angle, while

$$\chi_r(e_l) \equiv \arctan\left(-\frac{e_l(t)}{\Delta_l}\right) \tag{10}$$

is a velocity-path relative angle which ensures that velocity is directed toward a point on the path located a *lookahead distance* $\Delta_l > 0$ ahead of the direct projection of $p(t)$ onto the path, as shown in Figure 3. If a path is made up of n straight-line segments connected by $n+1$ waypoints, a strategy must be employed to purposefully switch between these segments as they are traversed. A so-called circle of acceptance in association with each waypoint, with $\mathrm{R}_{k+1} > 0$ for waypoint $k+1$, such that the corresponding switching criterion becomes

$$(x_{k+1} - x(t))^2 + (y_{k+1} - y(t))^2 \le \mathrm{R}_{k+1}^2 \tag{11}$$

A more suitable switching criterion may solely involve the along-track distance $s(t)$, such that if the total distance between waypoints p_k and p_{k+1} is denoted s_{k+1}, a switching is activated when $(s_{k+1} - s_k) \le \mathrm{R}_{k+1}$. This approach has the advantage that $p(t)$ does not need to enter the waypoint-enclosing circle for a switching to occur, that is, no restrictions are imposed on the cross-track error.

In the navigation system, the required hovercraft velocity (ν_{lpf}) is computed with the measured position and attitude (η) in the following way: The time derivative of η is computed and then the hovercraft velocity (ν) in the body fixed frame is calculated using (1). It is low pass filtered to come out as ν_{lpf}, which is used in control system.

B. Control

With the desired surge speed (u_d) and yaw angle (ψ_d) from the guidance system, the NN based adaptive dynamic inversion control is designed. The directly controlled dynamics (surge and sway) follow from (2)

$$\begin{aligned} \dot{u} + f_u + \Delta_u &= \tau_u \\ \dot{r} + f_r + \Delta_r &= \tau_r \end{aligned} \tag{12}$$

where the total control signals, τ_u and τ_r consist of the nominal control based on dynamic inversion and an adaptive control components:

$$\begin{aligned} \tau_u &= \tau_{u_n} + \tau_{u_{ad}} \\ \tau_r &= \tau_{r_n} + \tau_{r_{ad}} \end{aligned} \tag{13}$$

From (13), τ_u consists of a PI dynamic inversion nominal control and the adaptive control

$$\begin{aligned} \tau_{u_n} &= \dot{u}_d - K_{p_u}(u - u_d) - K_{i_u}\int_0^t (u - u_d)d\tau + f_u \\ \tau_{u_{ad}} &= \hat{\Delta}_u \end{aligned} \tag{14}$$

where u_d is the desired surge speed, K_{p_u} and K_{i_u} are positive PI gains, and $\hat{\Delta}_u$ is the estimate of the uncertainty (Δ_u) in the surge dynamics, which is described in detail, in the sequel. Also, from (13), τ_r consists of PID dynamic inversion nominal control and adaptive control

$$\begin{aligned} \tau\_r_n &= \dot{r}_d - K_{d_\psi}(r - r_d) - K_{p_\psi}(\psi - \psi_d) \\ &\quad - K_{i_\psi}\int_0^t (\psi - \psi_d)d\tau + f_r \\ \tau_{r_{ad}} &= \hat{\Delta}_r \end{aligned} \tag{15}$$

where ψ_d is desired yaw angle; $r_d = \dot{\psi}_d$ is its yaw rate; K_{p_ψ}, K_{i_ψ}, and $K_{d_\psi}$are positive PID gains; and $\hat{\Delta}_r$ is the estimate of the uncertainty (Δ_r) in the yaw dynamics, which will be described in detail.

In order to express the adaptive signals $\hat{\Delta}_u$ and $\hat{\Delta}_r$, the error dynamics of $\tilde{u}$ and $\tilde{\psi}$ are required. Substituting (14) into the surge dynamics in (12), the surge error dynamics follow

$$\dot{\tilde{u}} + K_{p_u}\tilde{u} + K_{i_u}\int_0^t \tilde{u}d\tau + \tilde{\Delta}_u = 0 \tag{16}$$

where $\tilde{u} = u - u_d$ and $\tilde{\Delta}_u = \Delta_u - \hat{\Delta}_u$. Also substituting (15) into the yaw dynamics in (12), yaw error dynamics follow

$$\ddot{\tilde{\psi}} + K_{d_\psi}\dot{\tilde{\psi}} + K_{p_\psi}\tilde{\psi} + K_{i_\psi}\int_0^t \tilde{\psi}(\tau)d\tau + \tilde{\Delta}_r = 0 \tag{17}$$

where $\tilde{\psi} = \psi - \psi_d$ and $\tilde{\Delta}_r = \Delta_r - \hat{\Delta}_r$. In state-space form, (16) can be written as

$$\dot{e}_u = A_u e_u + B_u \tilde{\Delta}_u \tag{18}$$

where $e_u = \left[\tilde{u}, \int_0^t \tilde{u}d\tau\right]^T$; $A_u < 0$ is *Hurwitz* with positive gains $K_{p_u} = 2\Lambda_u$, $K_{i_u} = {\Lambda_u}^2$, and $\Lambda_u > 0$; and

$$A_u = \begin{bmatrix} -K_{p_u} & -K_{i_u} \\ 1 & 0 \end{bmatrix}, B_u = \begin{bmatrix} -1 \\ 0 \end{bmatrix} \tag{19}$$

In state-space form, (17) can also be written as

$$\dot{e}_r = A_r e_r + B_r \tilde{\Delta}_r \tag{20}$$

where $e_r = \left[\dot{\tilde{\psi}}, \tilde{\psi}, \int_0^t \tilde{\psi}(\tau)d\tau\right]^T$; $A_r < 0$ is *Hurwitz* with positive gains $K_{p_\psi} = 3\Lambda_\psi^2$, $K_{i_u} = \Lambda_\psi^3$, $K_{d_\psi} = 3\Lambda_\psi$, and $\Lambda_\psi > 0$; and

$$A_r = \begin{bmatrix} -K_{d_\psi} & -K_{p_\psi} & -K_{i_\psi} \\ 1 & 0 & 0 \\ 0 & 1 & 0 \end{bmatrix}, B_r = \begin{bmatrix} -1 \\ 0 \\ 0 \end{bmatrix} \tag{21}$$

Equations (18) and (20) can be expressed in a compact form as

$$\dot{e} = Ae + B\tilde{\Delta} \tag{22}$$

where $e = [e_u^T, e_r^T]^T$; $A < 0$ is *Hurwitz*; and

$$A = \begin{bmatrix} A_u & 0_{2\times 3} \\ 0_{3\times 2} & A_r \end{bmatrix}, B = \begin{bmatrix} B_u & 0_2 \\ 0_3 & B_r \end{bmatrix}, \tilde{\Delta} = \begin{Bmatrix} \tilde{\Delta}_u \\ \tilde{\Delta}_r \end{Bmatrix} \tag{23}$$

The corresponding Lyapunov equation follows

$$A^T P + PA + Q = 0, Q = Q^T > 0 \tag{24}$$

Adaptive controls in (14) and (15) can be expressed as

$$\tau_{ad} = \left[\tau_{u_{ad}}^T, \tau_{r_{ad}}^T\right]^T = \widehat{W}^T(t)\beta(\nu, \psi) \tag{25}$$

where $\widehat{W}(t)$ comes from

$$\dot{\widehat{W}} = \Gamma\left(\beta(\nu, \psi)e^T PB - \widehat{W}_m\right) \tag{26}$$

where Γ is a positive adaptation gain, $\beta(\nu, \psi)$ is basis function, P is the solution of (24), and $\widehat{W}_m$ is a modification term, i.e. $\widehat{W}_m = \sigma\widehat{W}$ for σ-modfication [62] and $\widehat{W}_m = \lambda|e|\widehat{W}$ for e-modfication [63] with the positive damping rates of σ and λ. Figure 4 shows the overall architecture of the guidance and control routines. Reference model shown in Figure 4 low-pass-filters the guidance commands generated from the guidance block, with filter frequencies of Λ_u and Λ_ψ.

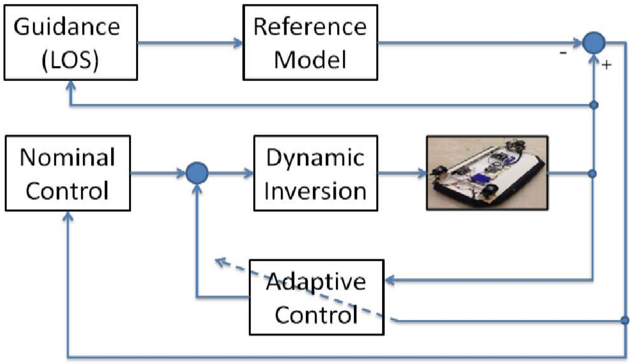

Figure 4. NN based Adaptive dynamic inversion control Architecture.

V. BOUNDEDNESS OF ERROR DYNAMICS

This section provides the uniformly ultimately boundedness (UUB) of the error signals in (22) with (23) and

$$\dot{\widetilde{W}} = \dot{W} - \dot{\widehat{W}} = -\Gamma\left(\beta(\mathrm{v},\psi)e^{T}PB - \widehat{W}_m\right) \tag{27}$$

where $\widetilde{W} = W - \widehat{W}$.

Theorem. Consider the nonlinear uncertain dynamic system in (3) and assume the linear parameterization in (5) to be hold. Furthermore consider the nominal dynamic inversion control in (14) and (15) and the adaptive control in (25) with weight update law in (26). Then, the closed error signals given by (22) and (27) are UUB for all $\left(e(0),\widetilde{W}(0)\right) \in D_{\mathrm{x}}$.

Proof. Consider the following Lyapunov candidate function

$$V\left(e,\widetilde{W}\right) = e^{T}Pe + \Gamma^{-1}\mathrm{tr}\left[\widetilde{W}^{T}\widetilde{W}\right] \tag{28}$$

With the error dynamics in (22) and (27), the time derivate of (28) can be written as

$$\begin{aligned}&\dot{V}\left(e,\widetilde{W}\right)\\ &= 2e^{T}P\left(Ae + B\tilde{\Delta}\right) - 2\mathrm{tr}\left[\widetilde{W}^{T}\left(\beta(\mathrm{v},\psi)e^{T}PB - \widehat{W}_m\right)\right]\end{aligned} \tag{29}$$

With the assumption in (5) and the Lyapunov equation in (24), (29) can be written as

$$\begin{aligned}&\dot{V}\left(e,\widetilde{W}\right)\\ &= -e^{T}Qe + 2e^{T}PB\varepsilon\\ &+ \underbrace{2e^{T}PB\widetilde{W}^{T}\beta(\mathrm{v},\psi) - 2\,\mathrm{tr}\left[\widetilde{W}^{T}\beta(\mathrm{v},\psi)e^{T}PB\right]}_{=0}\\ &+ 2\mathrm{tr}\left[\widetilde{W}^{T}\widehat{W}_m\right]\end{aligned} \tag{30}$$

Using Young's inequality [64], (30) with σ-modification can be written as

$$\begin{aligned}&\dot{V}\left(e,\widetilde{W}\right)\\ &\leq -e^{T}Qe + 2e^{T}PB\varepsilon - \sigma\,\mathrm{tr}\left[\widetilde{W}^{T}\widetilde{W}\right] + \sigma\,\mathrm{tr}\left[W^{T}W\right]\\ &\leq -\lambda_{\min}(Q)|e|^{2} - 2\|PB\|\epsilon|e| - \sigma\left\|\widetilde{W}\right\|_F^{2} + \sigma\|W\|_F^{2}\end{aligned} \tag{31}$$

Defining the followings

$$\begin{aligned}c &\equiv \lambda_{\min}(Q)\\ d &\equiv \|PB\|\epsilon\\ \mathbf{e}^{2} &\equiv \frac{\|PB\|^{2}\epsilon^{2}}{\lambda_{\min}(Q)} + \sigma\|W\|_F^{2}\end{aligned} \tag{32}$$

Equation (30) can be written as

$$\dot{V}\left(e,\widetilde{W}\right) \leq -c\left(|e| - \frac{d}{c}\right)^{2} - \sigma\left\|\widetilde{W}\right\|_F^{2} + \mathbf{e}^{2} \tag{33}$$

Consequently, we can conclude that either of the following conditions:

$$|e| > \Psi_1,\ \left\|\widetilde{W}\right\|_F > \Psi_2 \tag{34}$$

render $\dot{V}\left(e,\widetilde{W}\right) < 0$, where $\Psi_1 = \frac{\mathbf{e}}{\sqrt{c}} + \frac{d}{c}$ and $\Psi_2 = \frac{\mathbf{e}}{\sqrt{\sigma}}$, and it follows that $|e|$ and $\left\|\widetilde{W}\right\|_F$ are UUB.

In similar manner, e-modification in (25) replaces (33) with

$$\dot{V}\left(e,\widetilde{W}\right) \leq -|e|\left(d_1|e| + \lambda\left\|\widetilde{W}\right\|_F^{2} - d_2\right) \tag{35}$$

where $d_1 = \lambda_{\min}(Q)$, $d_2 = -2\|PB\|\epsilon + \lambda\|W\|_F^{2}$ and makes $\dot{V}\left(e,\widetilde{W}\right)$ negative as long as the term in the braces is positive. Therefore, the following conditions:

$$|e| > \frac{d_2}{d_1},\ \left\|\widetilde{W}\right\|_F > \sqrt{\frac{d_2}{\lambda}} \tag{36}$$

renders $\dot{V}\left(e,\widetilde{W}\right) < 0$, and it follows that $|e|$ and $\|W\|_F^{2}$ are UUB. ■

VI. ILLUSTRATIVE SIMULATION

The vehicle's mass $m = 11.07$ $[kg]$, the rotational mass moment of inertia $J = 1.59$ $[kg \times m^{2}]$, the coefficients of viscous and rotational friction $d_v = 4.6$ and $d_r = 0.75$, and the moment arm $l = 0.254$ $[m]$ are selected parameter values for simulation. The initial conditions of hovercraft are $(x,y,\psi,u,v,r) = (0,0,0,0,0,0)$. For the GNC design, the circle of acceptance (R_k) is fixed as 1[m], the desired surge speed ($u_d = 0.15$ $[m/s]$) and heading angle (ψ_d) are low-pass-filtered with filter frequencies of $\Lambda_u = 0.4$ and $\Lambda_\psi = 0.7$ [rad/sec], respectively, which make the dynamic inversion control signals, τ_{u_n} and τ_{r_n} in (13) and (14), respectively.

The error dynamics (21) also consists of Λ_u and Λ_ψ and the Lyapunov solution P in (23) can be calculated with $Q = I_5$

$$P = \begin{bmatrix} 3.2250 & 3.1250 & & 0_{2\times 3} & \\ 3.1250 & 4.5312 & & & \\ & & 3.0991 & 3.5983 & 1.4577 \\ & 0_{3\times 2} & 3.5983 & 6.6985 & 2.7879 \\ & & 1.4577 & 2.7879 & 1.5657 \end{bmatrix} \tag{37}$$

For the NN estimated weight update law in (25), the adaptation gain $\Gamma = 20$, e-modificatin damping gain $\lambda = 30$, and the basis function are used with a bias term and six sigmoidal basis functions $\beta_i(x_i)$ as written in (38)

$$\beta_i(x) = \begin{cases} 5 & ,i = 1 \\ \frac{1-e^{-ax_i}}{1+e^{-ax_i}} & ,i = 2,3,\ldots,7 \end{cases} \tag{38}$$

where activation potential $a = 3$ and normalized $x_i = [\bar{u},\bar{v},\bar{r},\bar{v}\bar{r},\bar{u}\bar{r},\bar{u}\bar{v}]$ with $\bar{u} = \frac{u}{0.2}$, $\bar{v} = \frac{v}{0.2}$, and $\bar{r} = \frac{r}{0.2}$.

The test case is to follow eight waypoints as shown in Figure 5. The dynamic inversion control scheme (the nominal controller) was tested with and without the NN-based adaptation. The tests were conducted with and without external disturbances. The disturbances follow the sine waves of magnitude 0.5 [m/s^2] and frequency 1.0 [Hz] same in the surge and yaw control channels. Figures 5 to 7 show the performance of the control scheme in following waypoints, heading angle, and surge speed. The desired waypoints path, heading angle, and surge speed are shown with the black solid line. The nominal controller performance in the case of no external disturbances is shown with the red dash-dot line whereas its performance with external disturbances is shown with the blue dashed line. The black dotted line shows the performance of the NN based adaptive controller with external disturbances. Although the hovercraft follows the waypoints more or less in all cases as shown in Figure 5, the performance differences between the nominal and adaptive controllers are highlighted in Figures 6 and 7. With the NN based adaptation, the control scheme performs almost as well as the nominal controller with no external disturbances.

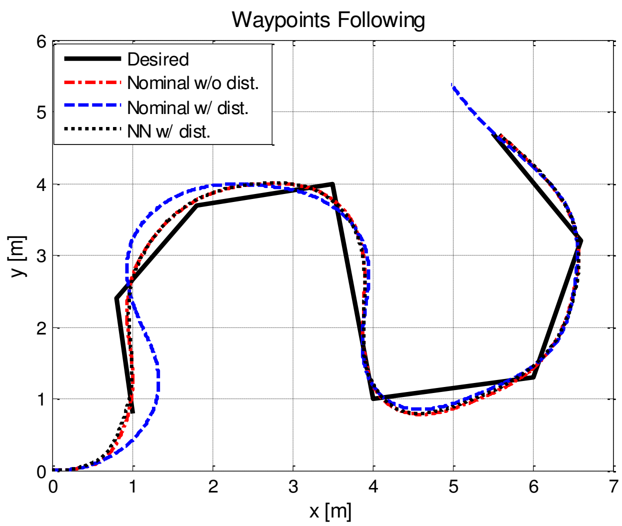

Figure 5. Performance of waypoints following.

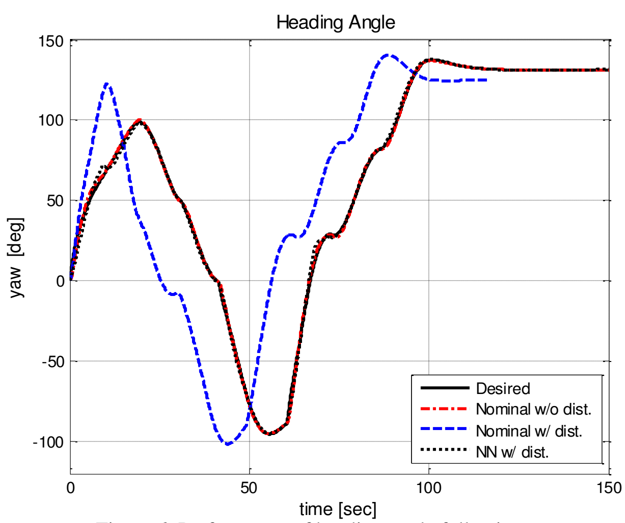

Figure 6. Performance of heading angle following.

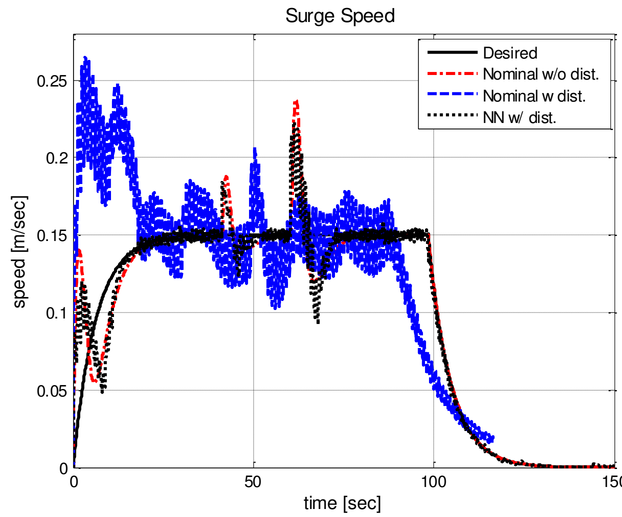

Figure 7. Performance of surge speed following.

VII. Conclusions

Current interest in autonomous systems is driving research for the development, testing and eventual application of such novel systems in a variety of domains. Modeling, guidance, navigation, and control technologies are required to assure that these platforms can perform safely, reliably and robustly in the presence of uncertainties and disturbances. There is a recognized need to improve the autonomy attributes of these vehicles. This paper introduced guidance, navigation, and control methods as applied to an underactuated hovercraft. An integrated approach was suggested to account for modeling and simulation. Additional studies are aimed to improve further autonomy attributes via fault diagnosis, failure prognosis and fault-tolerant control methods.

Acknowledgment

We gratefully acknowledge the support to this effort from the Office of Naval Research, NASA's Ames Research Center, and Impact Technologies.

References

[1] I. Fantoni, R. Lozano, F. Mazenc, and K. Y. Petterson, "Stabilization of a nonlinear underactuated hovercraft," *International Journal of Robust and Nonlinear Control,* vol. 10, pp. 645-654, Jul 15 2000.

[2] M.-C. Laiou and A. Astolfi, "Discontinuous control of high-order generalized chained systems," *Systems & Control Letters,* vol. 37, pp. 309-322, 1999.

[3] L. C. McNinch, H. Ashrafiuon, and K. R. Muske, "Sliding mode setpoint control of an underactuated surface vessel: Simulation and experiment," in *American Control Conference (ACC), 2010*, 2010, pp. 5212-5217.

[4] M. Reyhanoglu, "Control and stabilization of an underactuated surface vessel," in *Decision and Control, 1996., Proceedings of the 35th IEEE Conference on*, 1996, pp. 2371-2376 vol.3.

[5] M. Reyhanoglu, "Exponential stabilization of an underactuated autonomous surface vessel," *Automatica,* vol. 33, pp. 2249-2254, 1997.

[6] W. Dong and Y. Guo, "Global time-varying stabilization of underactuated surface vessel," *Automatic Control, IEEE Transactions on,* vol. 50, pp. 859-864, 2005.

[7] T. Kim, T. Basar, and I. Ha, "Asymptotic stabilization of an underactuated surface vessel via logic-based control," in *American Control Conference, 2002. Proceedings of the 2002*, 2002, pp. 4678-4683 vol.6.

[8] F. Mazenc, K. Pettersen, and H. Nijmeijer, "Global uniform asymptotic stabilization of an underactuated surface vessel," *Automatic Control, IEEE Transactions on,* vol. 47, pp. 1759-1762, 2002.

[9] K. Y. Pettersen and O. Egeland, "Exponential stabilization of an underactuated surface vessel," in *Decision and Control, 1996., Proceedings of the 35th IEEE Conference on*, 1996, pp. 967-972 vol.1.

[10] K. Y. Pettersen and O. Egeland, "Robust control of an underactuated surface vessel with thruster dynamics," *Proceedings of the 1997 American Control Conference, Vols 1-6,* pp. 3411-3415, 1997.

[11] K. Y. Pettersen and T. I. Fossen, "Underactuated ship stabilization using integral control: Experimental results with cybership I," *Nonlinear Control Systems Design 1998, Vols 1& 2,* pp. 125-130, 1998.

[12] K. Y. Pettersen and T. I. Fossen, "Underactuated dynamic positioning of a ship - Experimental results," *Ieee Transactions on Control Systems Technology,* vol. 8, pp. 856-863, Sep 2000.

[13] K. Y. Pettersen, F. Mazenc, and H. Nijmeijer, "Global uniform asymptotic stabilization of an underactuated surface vessel: experimental results," *Control Systems Technology, IEEE Transactions on,* vol. 12, pp. 891-903, 2004.

[14] K. Y. Pettersen and H. Nijmeijer, "Global practical stabilization and tracking for an underactuated ship - A combined averaging and backstepping approach," *Modeling Identification and Control,* vol. 20, pp. 189-199, Oct 1999.

[15] D. Soro and R. Lozano, "Semi-global practical stabilization of an underactuated surface vessel via nested saturation controller," in *American Control Conference, 2003. Proceedings of the 2003*, 2003, pp. 2006-2011 vol.3.

[16] Y.-P. Tian and S. Li, "Smooth exponential stabilization of nonholonomic systems via time-varying feedback," in *Decision and Control, 2000. Proceedings of the 39th IEEE Conference on*, 2000, pp. 1912-1917 vol.2.

[17] Y.-P. Tian and S. Li, "Exponential stabilization of nonholonomic dynamic systems by smooth time-varying control," *Automatica,* vol. 38, pp. 1139-1146, 2002.

[18] A. P. Aguiar and J. P. Hespanha, "Position tracking of underactuated vehicles," in *American Control Conference, 2003. Proceedings of the 2003*, 2003, pp. 1988-1993 vol.3.

[19] H. Ashrafiuon, K. R. Muske, L. C. McNinch, and R. A. Soltan, "Sliding-Mode Tracking Control of Surface Vessels," *Industrial Electronics, IEEE Transactions on,* vol. 55, pp. 4004-4012, 2008.

[20] A. Behal, D. M. Dawson, W. E. Dixon, and Y. Fang, "Tracking and regulation control of an underactuated surface vessel with nonintegrable dynamics," *Ieee Transactions on Automatic Control,* vol. 47, pp. 495-500, Mar 2002.

[21] A. Behal, D. M. Dawson, B. Xian, and P. Setlur, "Adaptive tracking control of underactuated surface vessels," *Proceedings of the 2001 Ieee International Conference on Control Applications (Cca'01),* pp. 645-650, 2001.

[22] S. P. Berge, K. Ohtsu, and T. I. Fossen, "Nonlinear control of ships minimizing the position tracking errors," *Modeling Identification and Control,* vol. 20, pp. 177-187, Jul 1999.

[23] K. C. Cao and Y. P. Tian, "A time-varying cascaded design for trajectory tracking control of non-holonomic systems," *International Journal of Control,* vol. 80, pp. 416-429, 2007/03/01 2007.

[24] K. D. Do, Z. P. Jiang, and J. Pan, "Robust global stabilization of underactuated ships on a linear course: State and output feedback," *International Journal of Control,* vol. 76, pp. 1-17, 2003/01/01 2003.

[25] K. D. Do and J. Pan, "Global tracking control of underactuated ships with nonzero off-diagonal terms in their system matrices," *Automatica,* vol. 41, pp. 87-95, 2005.

[26] M. A. G. Indiveri, and G. Casalino, "Nonlinear time-invariant feedback control of an underactuated marine vehicle along a straight course," in *In Proceedings of the 2000 Conference on Maneuvering and Control of Marine Craft*, 2000, pp. 221–226.

[27] J. M. Godhavn, "Nonlinear tracking of underactuated surface vessels," in *Decision and Control, 1996., Proceedings of the 35th IEEE Conference on*, 1996, pp. 975-980 vol.1.

[28] Z.-P. Jiang, "Global tracking control of underactuated ships by Lyaounov's direct method," *Automatica,* vol. 38, pp. 301-309, 2002.

[29] E. Lefeber, K. Y. Pettersen, and H. Nijmeijer, "Tracking control of an underactuated ship," *Control Systems Technology, IEEE Transactions on,* vol. 11, pp. 52-61, 2003.

[30] K. Y. Pettersen and H. Nijmeijer, "Tracking control of an underactuated surface vessel," in *Decision and Control, 1998. Proceedings of the 37th IEEE Conference on*, 1998, pp. 4561-4566 vol.4.

[31] K. Y. Pettersen and H. Nijmeijer, "Underactuated ship tracking control: theory and experiments," *International Journal of Control,* vol. 74, pp. 1435-1446, Sep 2001.

[32] G. J. Toussaint, T. Basar, and F. Bullo, "H_inf-optimal tracking control techniques for nonlinear underactuated systems," in *Decision and Control, 2000. Proceedings of the 39th IEEE Conference on*, 2000, pp. 2078-2083 vol.3.

[33] G. J. Toussaint, T. Basar, and F. Bullo, "Tracking for nonlinear underactuated surface vessels with generalized forces," *Proceedings of the 2000 Ieee International Conference on Control Applications,* pp. 355-360, 2000.

[34] G. J. Toussaint, T. Basar, and F. Bullo, "Motion planning for nonlinear underactuated vehicles using H-infinity techniques," *Proceedings of the 2001 American Control Conference, Vols 1-6,* pp. 4097-4102, 2001.

[35] M. Burger, A. Pavlov, E. Borhaug, and K. Y. Pettersen, "Straight line path following for formations of underactuated surface vessels under influence of constant ocean currents," in *American Control Conference, 2009. ACC '09.*, 2009, pp. 3065-3070.

[36] K. D. Do, Z. P. Jiang, and J. Pan, "Robust adaptive path following of underactuated ships," *Automatica,* vol. 40, pp. 929-944, 2004.

[37] K. D. Do and J. Pan, "Robust path-following of underactuated ships: Theory and experiments on a model ship," *Ocean Engineering,* vol. 33, pp. 1354-1372, 2006.

[38] K. D. Do and J. Pan, "Global robust adaptive path following of underactuated ships," *Automatica,* vol. 42, pp. 1713-1722, Oct 2006.

[39] E. Fredriksen and K. Y. Pettersen, "Global -exponential way-point maneuvering of ships: Theory and experiments," *Automatica,* vol. 42, pp. 677-687, 2006.

[40] I. A. F. Ihle, R. Skjetne, and T. I. Fossen, "Output feedback control for maneuvering systems using observer backstepping," *2005 IEEE International Symposium on Intelligent Control & 13th Mediterranean Conference on Control and Automation, Vols 1 and 2,* pp. 1512-1517, 2005.

[41] Z. Li, J. Sun, and S. Oh, "Path following for marine surface vessels with rudder and roll constraints: An MPC approach," in *American Control Conference, 2009. ACC '09.*, 2009, pp. 3611-3616.

[42] L. Moreira, T. I. Fossen, and C. Guedes Soares, "Path following control system for a tanker ship model," *Ocean Engineering,* vol. 34, pp. 2074-2085, 2007.

[43] R. Skjetne and T. I. Fossen, "Nonlinear maneuvering and control of ships," in *In Proceedings of MTS/IEEE OCEANS 2001*, 2001, pp. 1808–1815.

[44] R. Skjetne, O. N. Smogeli, and T. I. Fossen, "A Nonlinear Ship Manoeuvering Model: Identification and adaptive control with experiments for a model ship," *Modeling Identification and Control,* vol. 25, pp. 3-27, Jan 2004.

[45] A. J. Sørensen, S. I. Sagatun, and T. I. Fossen, "Design of a dynamic positioning system using model-based control," *Control Engineering Practice,* vol. 4, pp. 359-368, 1996.

[46] K. R. M. L. C. McNinch, and H. Ashrafiuon., "Model-based predictive control of an unmanned surface vessel," in *In Proceedings of the 11th IASTED International Conference on Intelligent Systems and Control*, 2008, pp. 385–390.

[47] R. Skjetne, T. I. Fossen, and P. V. Kokotović, "Robust output maneuvering for a class of nonlinear systems," *Automatica,* vol. 40, pp. 373-383, 2004.

[48] A. Isidori, *Nonlinear Control Systems*. Berlin: Springer-Verlag, 1989.

[49] G. Meyer and L. Cicolani, "Application of Nonlinear Systems Inverses to Automatic Flight Control Design—System Concepts and Flight Evaluations. Theory and Applications of Optimal Control in Aerospace Systems, AGARDograph No. 251, July 1981. Center, MS 210-3, FTS-5446."

[50] P. Menon, G. Chatterji, and V. Cheng, "A two-time-scale autopilot for high-performance aircraft," in *AIAA, Guidance, Navigation and Control Conference, New Orleans, LA*, 1991, p. 1991.

[51] J. M. Buffington, A. G. Sparks, and S. S. Banda, "Full conventional envelope longitudinal axis flight control with thrust vectoring," in *American Control Conference, 1993*, 1993, pp. 415-419.

[52] D. Bugajski, D. Enns, and M. Elgersma, "A dynamic inversion based control law with application to the high angle-of- attack research

vehicle," in *AIAA Guidance, Navigation and Control Conference, Portland, OR*, 1990, pp. 826-839.

[53] S. A. Snell, D. ENNS, W. GARRARD, and J. A M L, "Nonlinear inversion flight control for a supermaneuverable aircraft," *Journal of Guidance, Control, and Dynamics,* vol. 15, p. 3315, 1992.

[54] J. S. Brinker and K. A. Wise, "Stability and flying qualities robustness of a dynamic inversion aircraft control law," *Journal of guidance, control, and dynamics,* vol. 19, 2012.

[55] R. J. Adams and S. S. Banda, "An integrated approach to flight control design using dynamic inversion and μ-synthesis," in *American Control Conference, 1993*, 1993, pp. 1385-1389.

[56] J. Buffington, R. Adams, and S. Banda, "Robust, nonlinear, high angle-of-attack control design for a supermaneuverable vehicle," in *AIAA Guidance, Navigation and Control Conference, Monterey, CA*, 1993, pp. 690-700.

[57] M. S. K. Hornik, and H. White, "Multilayer Feedforward Networks are Universal Approximators," *Neural Networks,* vol. 2, pp. 359-366, 1989.

[58] R. M. Sanner and J. J. E. Slotine, "Gaussian networks for direct adaptive control," *Neural Networks, IEEE Transactions on,* vol. 3, pp. 837-863, 1992.

[59] S. S. Sastry and A. Isidori, "Adaptive control of linearizable systems," *Automatic Control, IEEE Transactions on,* vol. 34, pp. 1123-1131, 1989.

[60] I. Kanellakopoulos, P. V. Kokotovic, and A. S. Morse, "Systematic design of adaptive controllers for feedback linearizable systems," *Automatic Control, IEEE Transactions on,* vol. 36, pp. 1241-1253, 1991.

[61] M. Breivik and T. I. Fossen, "Guidance laws for planar motion control," in *Decision and Control, 2008. CDC 2008. 47th IEEE Conference on*, 2008, pp. 570-577.

[62] P. A. Ioannou and P. V. Kokotovic, "Instability analysis and improvement of robustness of adaptive control," *Automatica,* vol. 20, pp. 583-594, 1984.

[63] K. Narendra and A. Annaswamy, "A new adaptive law for robust adaptation without persistent excitation," *Automatic Control, IEEE Transactions on,* vol. 32, pp. 134-145, 1987.

[64] D. S. Bernstein, *Matrix mathematics: theory, facts, and formulas*: Princeton University Press, 2009.